Novel Transform for Ultra Wide-Band Radar Imaging with Circular Scanning Antennas

Takuya Sakamoto*, Toru Sato,
Graduate School of Informatics
Kyoto University
Yoshida-Honmachi, Sakyo-ku
Kyoto 606-8501, Japan

Rahmi Salman, Ingolf Willms,
Fachgebiet Nachrichtentechnische Systeme
Universitat Duisburg-Essen
Duisburg, Germany

Alexander G. Yarovoy
Microwave Sensing, Signals and Systems
Delft University of Technology
Mekelweg 4, 2628 CD
Delft, the Netherlands

***Abstract*—Short-range imaging technology using ultra wide-band radar is increasingly seen as an essential modality in a variety of applications. Of those, security-related systems require fast computation and real-time operation. Many conventional radar imaging methods trade-off computational speed and imaging quality. The revised range point migration method is known to be both fast and accurate, resolving the issues associated with trade-off. However, this method can be applied only to an antenna scanning along a straight line or in a plane. For various applications it is more practical to assume a circular scanning trajectory, a circular antenna array, or a rotating target. For that development, we derive a new transform in polar coordinates for ultra wide-band radar imaging and create a corresponding fast imaging algorithm that processes received signals into target shapes. The performance of this imaging algorithm is demonstrated in an application to measurement data. The fast and accurate imaging capability is established by the experimental results.**

I. Introduction

To complement existing camera-based systems, ultra-wide-band (UWB) radar imaging technology has been widely used in security-related applications, such as concealed weapon detection and surveillance systems, and in autonomous rescue robotics. One necessary feature for UWB radar imaging in such applications is computational speed because real-time operations are needed with a high frame-rate to capture fast moving targets and changing situations. A variety of imaging methods for UWB radars have been developed [1], [2], [3], [4], [5], [6]. However, many of these existing imaging methods do not fulfill fast computing criteria.

One proposal developed to meet this need was SEABED (shape estimation algorithm based on the boundary scattering transform (BST) and extraction of directly scattered waves) [7], [8], [9], [10], which uses a reversible transform, BST (inverse boundary scattering transform) that depicts the relationship between target shape and received signals obtained with an antenna scanning along a straight line or flat plane. The revised range point migration (RRPM) method, which is an extension of the SEABED method, can obtain images even for complex-shaped targets under noisy condition [11], [12]. However, in practice, antennas scanning on a circle, circular sensor arrays or a fixed antenna with rotating targets are more commonly used because such systems can cover the whole target surface.

To apply the SEABED method to circular antenna scanning scenarios, Helbig et al. proposed another transform for imaging with arbitrary scanning trajectories by approximating the scanning surface with a tangent plane [13]. However, an accurate transform without approximation is indispensable if it is to be applied in the RRPM with circular coordinates because the RRPM method calculates derivatives of the quasi-wavefronts using multiple peak points in the neighborhood of a point of interest.

Below, we report about a new transform that maps received signals into the target shapes from a circular antenna scanning trajectory. Incorporating the modified RRPM for the polar coordinates, we develop a new algorithm that is capable of obtaining images even for complex-shaped targets. We conducted measurements using maximum length binary sequence (m-sequence) UWB radar system and a metallic target on a rotating platform to assess the performance of the proposed method.

II. System Model

We employ 2-dimensional polar coordinates in the imaging plane for our UWB radar system. Fig. 1 shows a schematic of the system model. The radar is a mono-static system that has only a single antenna used as both transmitter and receiver. The antenna is positioned on a ring of radius R, centered on the origin of the coordinate system. With azimuth angle θ, the location of the antenna is expressed as $(x, y) = (R\cos\theta, R\sin\theta)$. Targets are placed within this circular trajectory of the scanning antenna. UWB pulses are transmitted and echoes are received. The received signals contain not only echoes from the target but also a coupling signal and background clutter. To eliminate these unnecessary signals, the background signal, measured without a target prior to actual measurement, can be subtracted from the received signal. Given the antenna location corresponding to the angle θ, the received signal is denoted by $s(\theta, r)$ with $r = ct/2$, where c is the speed of the electromagnetic wave and t the time interval between transmission and reception.

III. Quasi-Wavefront Extraction

To estimate the target shape, many of the conventional imaging methods use back propagation to form an image. These

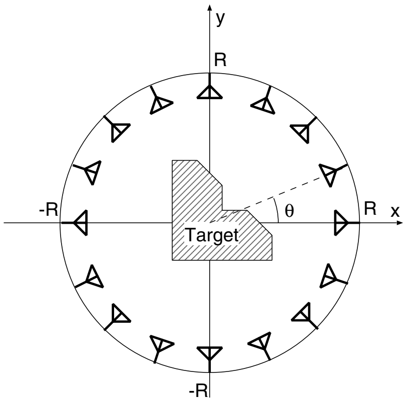

Fig. 1. System model with a circular antenna array surrounding a target.

are also called migration. Its processing is time-consuming because the propagation paths need to be calculated repeatedly. To overcome this difficulty, we developed a fast imaging algorithm using the reversible boundary scattering transform (BST) between target shape and received signals. To apply it to circular antenna scanning trajectory, below this BST is adapted to the polar coordinates of the imaging plane.

First, we extract peaks of the received signals, which satisfy

$$\frac{\partial}{\partial r} s(\theta, r) = 0, \tag{1}$$

$$|s(\theta, r)| > T_{\mathrm{s}}, \tag{2}$$

where T_{s} is a constant threshold introduced to filter out noise. These peaks are indexed as (θ_i, r_i) for $(i = 1, 2, \cdots, N)$. The corresponding amplitudes of these peaks are, for simplicity, denoted $s_i = s(\theta_i, r_i)$. For a single simple-shaped target, these points are easily connected sequentially to form curved lines $r(\theta)$. The resulting function is called a quasi-wavefront.

IV. Novel Transform for Polar Coordinates

We assume a metallic target that has a clear boundary between background and target media. In this case, scattering occurs on this boundary. Our purpose in this paper is to estimate the shape of the boundary, not the permittivity of the target.

In the previous section, we calculated a function $r(\theta)$ that gives the distance between the antenna and the scattering point on the boundary. The target boundary is expressed in the polar coordinates as

$$\begin{pmatrix} x \\ y \end{pmatrix} = R \begin{pmatrix} \cos\theta \\ \sin\theta \end{pmatrix} + r(\theta) \begin{pmatrix} \cos\phi \\ \sin\phi \end{pmatrix}, \tag{3}$$

where ϕ is the angle of the scattering point as seen from the antenna. For simplicity, we rotate the coordinates by $-\theta$ to set the antenna position at $(x, y) = (R, 0)$. The actual target boundary satisfies the condition

$$\frac{\mathrm{d}}{\mathrm{d}\theta} \begin{pmatrix} x(\theta) \\ y(\theta) \end{pmatrix} = 0. \tag{4}$$

Therefore, the following equations must be satisfied simultaneously:

$$R \begin{pmatrix} 0 \\ -1 \end{pmatrix} = r \frac{\mathrm{d}\phi}{\mathrm{d}\theta} \begin{pmatrix} -\sin\phi \\ \cos\phi \end{pmatrix} + \frac{\mathrm{d}r}{\mathrm{d}\theta} \begin{pmatrix} \cos\phi \\ \sin\phi \end{pmatrix}, \tag{5}$$

where ϕ is a function of θ chosen so that the point expressed in Eq. (3) is on the target boundary.

By deleting $\mathrm{d}\phi/\mathrm{d}\theta$ from these equations, we obtain

$$\sin\phi = -\frac{\mathrm{d}r/\mathrm{d}\theta}{R}, \tag{6}$$

or equivalently

$$\cos\phi = -\sqrt{1 - \left(\frac{\mathrm{d}r/\mathrm{d}\theta}{R}\right)^2}. \tag{7}$$

Note that the negative sign $\cos\phi = -\sqrt{1 - \sin^2\phi}$ is adopted because the target is placed within the antenna scanning circle, as discussed in the system model above. Therefore, $\cos\phi$ for $\theta \simeq 0$ must be negative.

For general θ, ϕ is expressed as

$$\phi = -\sin^{-1}\left(\frac{\mathrm{d}r/\mathrm{d}\theta}{R}\right) + \theta. \tag{8}$$

As a result, if r and $\mathrm{d}r/\mathrm{d}\theta$ are measured, the target image can be calculated using Eqs. (3) and (8). In this way, the target can be imaged with this transform without any iteration, quicking image processing. We call the transform defined by Eqs. (3) and (8) the polar IBST (PIBST).

V. Revised Range Point Migration

The procedure described above is a polar coordinate version of the SEABED algorithm [7]. The significant issue of the SEABED algorithm is that the derivative $\mathrm{d}r/\mathrm{d}\theta$ is too sensitive to noise and interference. The whole process depends on the assumption that the quasi-wavefront $r(\theta)$ can be clearly estimated, while the actual measurement is prone to various undesirable effects such as noise, clutter, and interference between multiple scattering waves. This issue makes it difficult to apply the SEABED algorithm to complex-shaped targets under noisy conditions.

These difficulties are, however, inevitable in practical scenarios of security-related applications. Therefore, we developed a revised range point migration (RRPM) method to mitigate the instability of the SEABED method [11], [12]. In this section, we propose a modified RRPM for polar coordinates.

With a weighted average function, the relative orientation of the peaks around the i-th peak is estimated as:

$$\psi_i = \frac{\sum_{j \neq i} w_{i,j} \tan^{-1}\left(\frac{r_i - r_j}{\theta_i - \theta_j}\right)}{\sum_{j \neq i} w_{i,j}}, \tag{9}$$

where

$$w_{i,j} = |s_i s_j| \exp\left(-\frac{(\theta_i - \theta_j)^2}{\sigma_\theta^2} - \frac{(r_i - r_j)^2}{\sigma_r^2}\right) \tag{10}$$

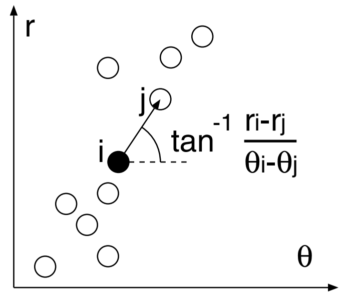

Fig. 2. Schematic of fast RPM method.

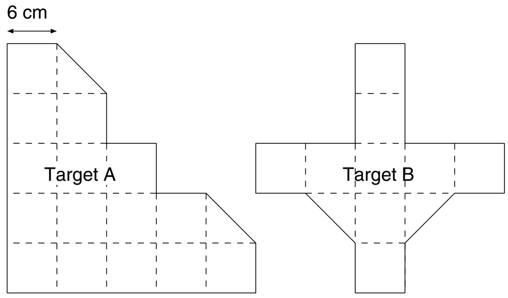

Fig. 3. Target shapes used in our measurements.

and $\left|\tan^{-1}\left(\frac{r_i-r_j}{\theta_i-\theta_j}\right)\right| < \pi/4$, and the summations are over pairs of peaks with the same sign in the 2nd derivative i. e.

$$s_{rr}(\theta_i, r_i)s_{rr}(\theta_j, r_j) > 0, \tag{11}$$

where $s_{rr} = \frac{\partial^2}{\partial r^2}s$. Figure 2 shows the schematic of the procedure in the RRPM method. As in this figure, the inclination of points around the i-th point is calculated by averaging the angle between the i-th and j-th points over all j close to the i-th point. By finding ψ_i using Eq. (9), we obtain an estimate of the quasi-wavefront orientation. We calculate the derivative $\mathrm{d}r/\mathrm{d}\theta|_{\theta=\theta_i} = \tan(\psi_i)$. Finally, we substitute r and $\mathrm{d}r/\mathrm{d}\theta$ to PIBST in Eqs. (3) and (8) to obtain the target image.

VI. Application to Measurement Data

We conduct measurements to investigate the performance of the proposed imaging algorithm. We used an m-sequence UWB radar [14], [15] with an operating band of DC-4.5 GHz. We combined this system with a 9 GHz carrier signal generator to up-convert and generate signals with a frequency band of 4.5 GHz to 13.5 GHz, with a bandwidth of 9 GHz giving a fractional bandwidth of 100%. In assembling a bi-static radar system, we mounted a pair of directive Teflon-embedded tapered slot line Vivaldi antennas [14], [16] with 10 cm of antenna separation to mitigate antenna cross-talk. The antenna gain is 15 dBi and the beam width is 25 degrees.

The target objects are metallic pillars with uniform horizontal cross-section (Fig. 3); the model is approximately considered to be two dimensional. Each target is placed in turn on a rotating platform whose axis is 100 cm away from the midpoint of the antennas, giving $R = 100.0$ cm. The table rotates 360 degrees in 1 degree steps, resulting in 360 measuring points. The rotation is electrically controlled with an accurate step motor. The detail of the measurement setup is given in [17] and [15]. The imaging has been performed for the same measurement data set using conventional imaging methods [14], [16], [17], [18]. We set the parameters for the proposed method as $T_s = 0.5A_{\max}$, $\sigma_\theta = 0.5°$ and $\sigma_r = 0.05$ cm, where $A_{\max}$ is the maximum amplitude of the signal. We extracted 5 quasi-wavefronts for each measurement angle.

For comparison, we first generated images using the conventional diffraction stack migration as in Figs. 4 and 5. The computation of the migration method took 20.9 s on average for these two targets. Figures 6 and 7 show the images

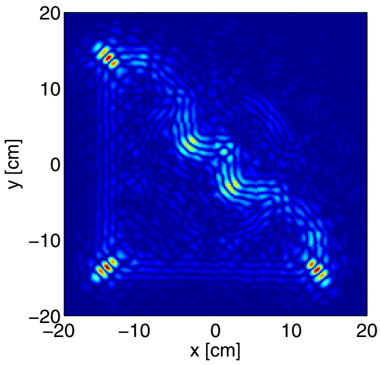

Fig. 4. Estimated target shape using the conventional migration method for target A.

generated using our proposed method. The results clearly show the imaging capability of the proposed method in obtaining imaging of these complex-shaped targets. The total imaging process of the proposed method took only 1.05 s, which is approximately 20 times shorter than using the conventional migration method. For comparing the computational times, we used a 64-bit Matlab 2012b running on a laptop with Intel Core i7-3610QM CPU with 2.30 GHz clock speed and 4.0 GB RAM. Although the imaging quality of the proposed method is not as good as the migration method, the outline of the target shapes are correctly estimated. Furthermore, the experimental investigation demonstrated the fast computational capability of the proposed method.

VII. Conclusion

In this paper, we proposed a new imaging algorithm for a UWB radar with circularly scanning antenna. The algorithm was developed by modifying the reversible transform IBST and deriving a new transform PIBST in polar coordinates. The transform requires the derivative of the delay time in terms of antenna orientation, which is susceptible to interference and noise. To resolve the instability associated with derivative estimates, we employed a modified RRPM described by polar coordinates to estimate a stable derivative. The performance of the proposed method has been investigated with measurements using a m-sequence radar system and metallic targets positioned on a rotating platform. The imaging results show

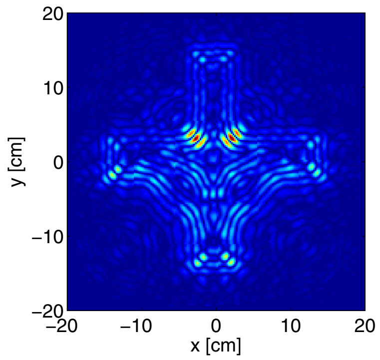

Fig. 5. Estimated target shape using the conventional migration method for target B.

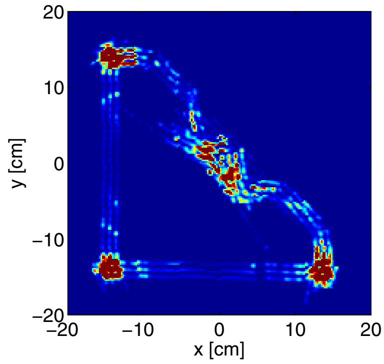

Fig. 6. Estimated target shape using the proposed method for target A.

that the proposed method is capable of obtaining images 20 times faster than the conventional migration method, indicating the immense potential of the proposed method in various applications.

ACKNOWLEDGEMENT

This study was supported in part by Japan Society for the Promotion of Science (JSPS) Postdoctoral Fellowships for Research Abroad (High-resolution imaging for human bodies with UWB radar using multipath echoes).

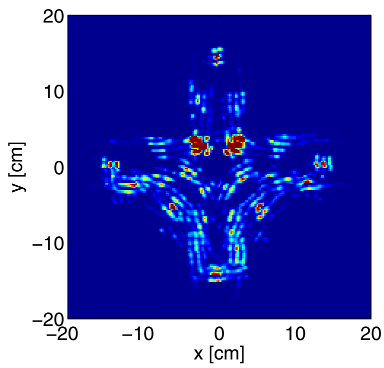

Fig. 7. Estimated target shape using the proposed method for target B.

REFERENCES

[1] X. Zhuge, A. G. Yarovoy, T. Savelyev, L. Ligthart, "Modified Kirchhoff migration for UWB MIMO array-based radar imaging" IEEE Transactions on Geoscience and Remote Sensing, vol. 48, no. 6, pp. 2692–2703, 2010.

[2] X. Zhuge, and A. Yarovoy, "A sparse aperture MIMO-SAR based UWB imaging system for concealed weapon detection," IEEE Transactions on Geoscience and Remote Sensing, vol. 49 no. 1, pp. 509–518, 2011.

[3] Y. Wang, Y. Yang, A. E. Fathy, "Experimental assessment of the cross coupling and polarization effects on ultra-wide band see-through-wall imaging reconstruction," IEEE MTT-S International Microwave Symposium Digest, pp. 9–12, June 2009.

[4] A. Nelander, "Switched array concepts for 3-D radar imaging," Proc. 2010 IEEE Radar Conference, pp. 1019–1024, 2010.

[5] T. Counts, A. C. Gurbuz, W. R. Scott Jr., J. H. McClellan, and K. Kim, "Multistatic ground-penetrating radar experiments," IEEE Trans. Geoscience and Remote Sensing, vol. 45, no. 8, pp. 2544–2553, Aug. 2007. 2008.

[6] Y. Yang and A. E. Fathy, "Development and implementation of a real-time see-through-wall radar system based on FPGA," IEEE Trans. Geoscience and Remote Sensing, vol. 47, no. 5, pp. 1270–1280, May 2009.

[7] T. Sakamoto, "A fast algorithm for 3-dimensional imaging with UWB pulse radar systems," IEICE Trans. on Communications, vol. E90-B, no. 3, pp. 636–644, 2007.

[8] S. Hantscher, A. Reisenzahn, C. G. Diskus, "Through-Wall Imaging With a 3-D UWB SAR Algorithm," IEEE Signal Processing Letters, vol. 15, pp. 269–272, 2008.

[9] R. Salman, I. Willms, "In-Wall Object Recognition based on SAR-like Imaging by UWB-Radar," Proc. 8th European Conference on Synthetic Aperture Radar (EUSAR), 2010.

[10] S. Kidera, Y. Kani, T. Sakamoto and T. Sato, "A fast and high-resolution 3-D imaging algorithm with linear array antennas for UWB pulse radars," IEICE Trans. on Communications, vol. E91-B, no. 8, pp. 2683–2691, 2008.

[11] T. Sakamoto, T. G. Savelyev, P. J. Aubry, and A. G. Yarovoy, "Revised Range Point Migration Method for Rapid 3-D Imaging with UWB Radar," Proc. 2012 IEEE International Symposium on Antennas and Propagation and USNC-URSI National Radio Science Meeting, July 2012.

[12] T. Sakamoto, T. G. Savelyev, P. J. Aubry, and A. G. Yarovoy, "Fast Range Point Migration Method for Weapon Detection using Ultra-Wideband Radar," Proc. European Radar Conference, Nov. 2012.

[13] M. Helbig, M. A. Hein, U. Schwarz, J. Sachs, "Preliminary investigations of chest surface identification algorithms for breast cancer detection," Proc. IEEE International Conference on Ultra-Wideband, pp. 195–198, Sep. 2008.

[14] R. Zetik, H. Yan, E. Malz, S. Jovanoska, G. Shen, R.S. Thomä, R. Salman, T. Schultze, R. Tobera, I. Willms, L. Reichardt, M. Janson, T. Zwick, W.Wiesbeck, T. Deißler, J. Thielecke, "Cooperative Localization and Object Recognition," UKoLoS Ultra-Wideband Radio Technologies for Communications, Localization and Sensor Applications, InTech Academic Publisher, ISBN: 978-953-307-740-6.

[15] R. Salman and I. Willms, "Super-Resolution Object Recognition Approach for Complex Edged Objects by UWB Radar," Object Recognition, Intech.

[16] R. Salman, I. Willms, L. Reichardt, T. Zwick and W. Wiesbeck, "On polarization diversity gain in short range UWB-Radar object imaging," Proc. 2012 IEEE International Conference on Ultra-Wideband, pp. 402–406, Sep. 2012.

[17] R. Salman and I. Willms, "3D UWB radar super-resolution imaging for complex objects with discontinous wavefronts," Proc. 2011 IEEE International Conference on Ultra-Wideband, Sep. 2011.

[18] R. Salman and I. Willms, "A mobile security robot equipped with UWB-radar for super-resolution indoor positioning and localisation applications," Proc. Indoor Positioning and Indoor Navigation, Nov. 2012.